



## **Full paper**

# **Experimental and numerical investigations on the robustness of dissipative joints**

T. Golea<sup>1</sup> | R. Carlevaris<sup>2</sup> | R. Tartaglia<sup>3</sup> | M. D’Aniello<sup>2</sup> | M. Latour<sup>4</sup> | V. Piluso<sup>4</sup> | J.-F. Démonceau<sup>1</sup>

### **Correspondence**

Eng. Tudor Golea  
University of Liège  
Urban and Environmental  
Engineering,  
Quartier Polytech 1, Allée de la  
découverte 9

Email: [tudor.golea@uliege.be](mailto:tudor.golea@uliege.be)

<sup>1</sup> University of Liège, Liège,  
Belgium

<sup>2</sup> University of Naples Federico II,  
Naples, Italy

<sup>3</sup> University of Sannio, Benevento,  
Italy

<sup>4</sup> University of Salerno, Salerno,  
Italy

### **Abstract**

Through previous research, experimental and numerical investigations performed on the innovative FREEDAM dissipative joints demonstrated the efficiency of these joints in moment-resisting frames in dissipating the seismic-induced energy. This paper presents additional experimental and numerical studies aimed at characterising the behaviour of FREEDAM joints up to failure for robustness-oriented design frameworks. Two real-scale beam-to-column joints were tested (i) under monotonic bending and (ii) under a virtual column loss scenario inducing bending moments and axial forces at the level of the tested joint. The experimental evidence emphasises the influence of the preload loss in the bolts clamping the sliding surfaces of the damper during the slippage of the joint, thus affecting both frictional and ultimate resistance. The tests confirmed the capacity of these joints to develop catenary action, ensuring significant displacement capacity under extreme loads. Numerical analyses were used to validate a simplified two-spring model (2SM) developed in previous studies. Different modelling strategies accounting for the loss of the bolt preload were assessed to ensure realistic characterisation of post-slippage behaviour—an essential aspect in robustness-related scenarios.

### **Keywords**

Dissipative joints, Experimental tests, Numerical analysis, Robustness.

## **1 Introduction**

Recent studies demonstrated the efficiency of innovative dissipative joints in seismic-resistant steel structures [1]. In the framework of Eurocodes, in addition to the rules and requirements provided in EN 1998-1 [2] to guarantee adequate seismic performance, EN 1991-1-7 [3] requires that any structure subjected to an exceptional event should not undergo damages disproportionate to the initiating cause, leading to additional requirements at the level of structural joints that are typically identified as key elements in case of such events.

The robustness of the dissipative FREE from DAMAge (FREEDAM) joints has been studied in previous RFCS research projects (FREEDAM and FREEDAM+) [1] relying on analytical and numerical tools partially validated against few experimental tests performed on scaled down specimens of these joints. Previous studies on steel frames equipped with FREEDAM joints demonstrated that the

response of these joints positively influences the structural performance under column loss scenarios [4], [5], [6]. However, findings from previous numerical and analytical studies [5] drew attention to the brittle failure expected to occur at the level of the dampers limiting the overall joint ductility.

Since a proper characterisation of the joints is paramount for assessing the structural robustness, this paper gives valuable insights on the full-range response of FREEDAM joints obtained through experimental testing. Real-scale double-sided joints were tested until failure under monotonic bending (Test 1) and a quasi-static virtual column loss scenario (Test 2).

The acquired experimental evidence allowed validating a mechanical model previously used for simulating these joints in global frame analyses [4], [5], and highlighted the particularities of the response of FREEDAM joints in robustness-related scenarios.

## 2 Experimental campaign

### 2.1 General description of the performed tests

Two experimental tests were conducted on real-scale double-sided beam-to-column FREEDAM joints assumed to be extracted from a moment-resisting frame (MRF) located on the perimeter of a pilot building currently under construction in the framework of the DREAMERS RFCS project. More precisely, the tested joint corresponds to an internal joint connecting the IPE450 beams to the HE400B columns of the 1<sup>st</sup> and 2<sup>nd</sup> floors of the perimeter frames as shown in Figure 1. Thus, the specimens consist of two IPE450 beams connected to a HE400B column through a FREEDAM connection (Device D1). S355 steel grade was used for structural members (i.e., beams and columns) and plate components of the dissipative joints with the only exception for the rib that was made of AISI304 stainless steel. The fasteners used to connect the different joint components are 10.9 grade bolts with varying diameters between M16 and M24.

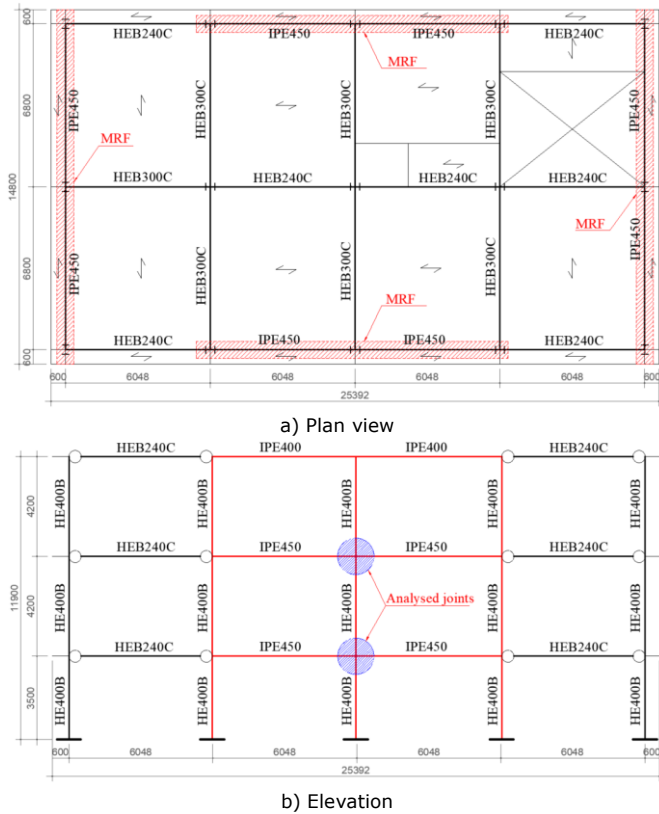


**Figure 1** Location of the studied joint within the DREAMERS structure

The performed tests aimed at characterising the full-range behaviour of FREEDAM joints under i) monotonic bending (Test 1) and ii) simultaneously applied bending moment and axial forces – loading conditions that mimic a hypothetical column loss scenario (Test 2). A quasi-static loading protocol was applied in both tests, thus allowing the execution of the experimental tests in a well-controlled manner with accurate and reliable “noise-free” recordings that provided valuable insights into the global response and local phenomena occurring within the FREEDAM joints.

### 2.2 Test setups and instrumentation

The test under monotonic bending (Test 1) was performed using a simple setup comprising an assembly of

restraining frames and a system of supports equipped with horizontal rollers to allow for horizontal movement of the specimen’s extremities. Lateral restraints were provided at 1.0 m from the column’s axis to prevent instabilities related to the lateral torsional buckling (LTB) of the beams observed in previous research [7] in tests performed under similar conditions. A hydraulic actuator of 2000 kN capacity and 400 mm stroke length was used to apply a vertical load at the stiffened top end of the column, as shown in Figure 2a.

As shown in Figure 2b, the setup for Test 2 consisted of an assembly of restraining frames and a horizontal in-plane restraining system comprising some transfer beams and columns anchored to the reinforced concrete floor of the lab. The latter allows transferring the beam membrane forces developed during testing to the reaction floor. Pinned connections that allow for frictionless in-plane rotations through a radial bearing and a pin were provided at the extremities of the specimen. The reaction frame supporting the hydraulic actuator as well as the frames providing the lateral restraints (in- and out-of-plane) were anchored to the reinforced concrete reaction floor using pretensioned high-strength anchor rods similar to Test 1.

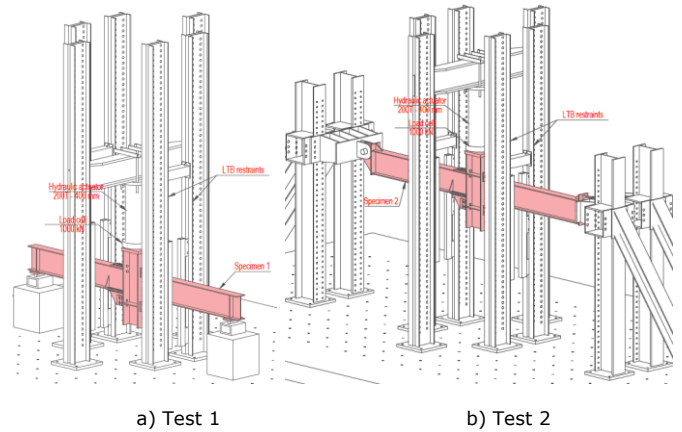


**Figure 2** 3D views of the test setups

During both tests, the vertically applied quasi-static load was continuously monitored using a load cell positioned between the actuator and the column head (loading plate). The load transfer to the column head was ensured by means of a load button with a convex contact surface, maintaining the alignment between the applied load and the column’s axis.

As indicated in Figure 3a, test specimen 1 was equipped with ten Linear Variable Displacement Transducers (LVDTs 01 to 10) used to measure the global displacements (vertical with LVDTs 01&02 and horizontal with LVDTs 09&10) and relative displacements (LVDTs 03-08) between the different parts of the connections. Additionally, to monitor the rotations of the beam-to-column connections as well as the potential in-plane tilt of the column, three inclinometers (IMs 01-03) were installed at the beams’ ends in the proximity of the FREEDAM joint and the column web.

Figure 3b shows the instrumentation used for capturing the response of the FREEDAM joint subjected to a virtual column loss during Test 2. In addition to the measurement instrumentation used for Test 1, two more LVDTs (11-12)

were provided at the mid-span of the beams to measure the vertical displacements. Two more inclinometers (IMs 04-05) were installed at the beam ends close to the lateral supports serving for estimating the potential horizontal displacements of the restraining system. Eighteen strain gauges (SG 01-18) were installed on the beams' flanges and webs serving for quantifying the membrane forces developing in the axially restrained beams.

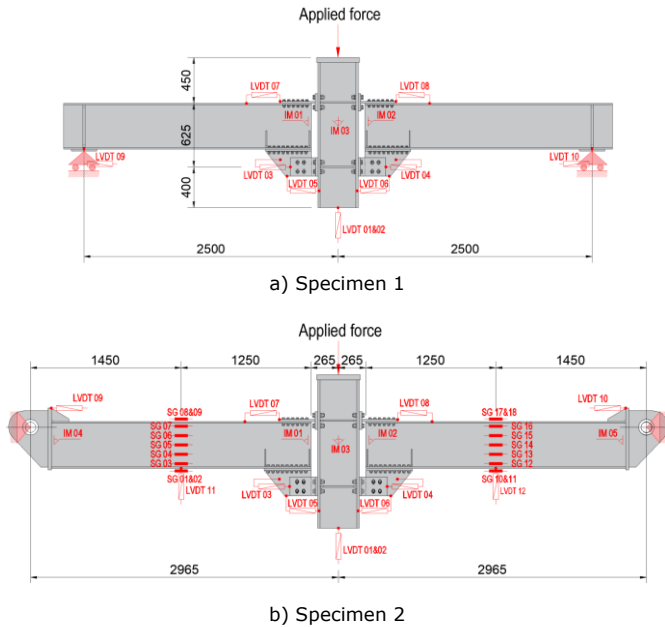


Figure 3 Tested specimens and measuring instrumentation

### 2.3 Material properties

The properties of steel material used in the constitutive parts of the test specimens were determined through tensile tests performed on coupons extracted from profiles/plates coming from the same production batch as the elements of the test specimens. Unfortunately, no coupons were available for the AISI304 haunch and the 10.9 grade bolts. Table 1 summarizes the mechanical characteristics of the tested materials according to ISO 6892-1:2019 [8].

Table 1 Mechanical properties from steel coupon tensile tests

Element	Region/ thickness	$R_{p0.2}$ (MPa)	$R_m$ (MPa)	$A$ (%)
<b>HE400B</b>	web	474.5	596	24.2
	flanges	415.4	571.3	30.9
<b>IPE450</b>	web	474.1	595.9	24.7
	flanges	456.4	587.8	27.5
<b>Plate 25</b>	25 mm	389.6	558.6	33.6
<b>Plate 20</b>	20 mm	426.8	514.6	34.4

### 2.4 Experimental results

Figure 4 shows the experimental results in terms of applied force vs. vertical displacement measured during Test 1. The experimental curve along with real-time

observations of the specimen response indicate that the sliding resistance of the two connections (left and right) was not reached simultaneously.

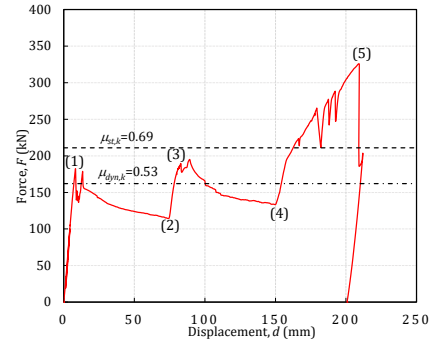


Figure 4 Test 1: Vertical load vs. displacement curve

In fact, the results reveal that there was a 7% difference between the sliding resistances of the two connections. The slippage in the right connection was initiated at an applied vertical force of approximately 182 kN, whereas the left connection reached its sliding resistance at approximately 195 kN applied load. This discrepancy may come from the slight variation of the preload applied to the damper bolts as well as from small differences in the coating of the friction pads and the contact with the other plate components of the damper (haunch and L-stubs). The sliding resistances of both connections fall in the range between the two design predictions, corresponding to the characteristic dynamic and static friction coefficients  $\mu_{dyn,k}=0.53$  and  $\mu_{st,k}=0.69$  corresponding to the friction pads coating material.

Unfortunately, the in-plane rotation of the column could not be restrained due to the impossibility of monitoring the horizontal in-plane reactions that would arise at the level of such restraints. This fact, in combination with the dissimilarity between the sliding resistance of both connections, induced a strong asymmetric response marked by 5 distinct phases governed by the successive slippage in the connections as suggested in Figures 4-5.

The failure occurred at the level of the damper bolts in the left connection (bolt fracture in shear). The test was stopped due to safety considerations, yet the brittle failure of the bottom bolt in shear and the excessive plastic deformations at the level of the other bolts active in bearing in the dampers indicate that the ultimate capacity of the joint was reached at 326 kN.

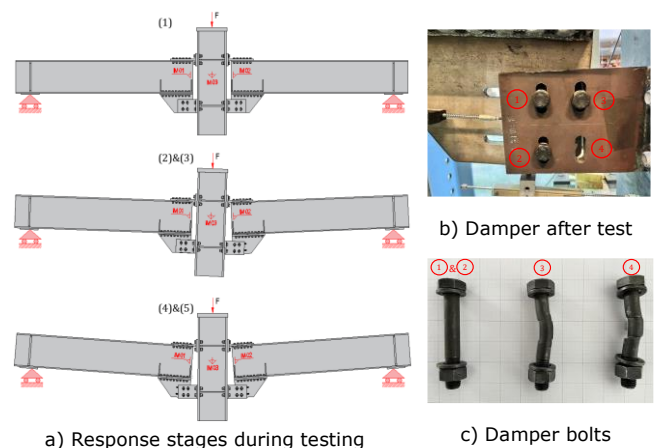


Figure 5 Test 1: response stages and observed failure of the specimen

Similar observations can be made for the response of test specimen 2. Due to the presence of tensile forces in the beams, the slippage occurred at lower values of the applied vertical load compared to the joint subjected to bending moment (and shear force) only. The shape of the curve as well as real-time observations indicate that a small difference in terms of slippage resistance between the two connections induced once again an asymmetric behaviour. Overall, the experimental response can be characterised by 5 distinct stages similar to Test 1.

Although a failure mode identical to the one observed in Test 1 was expected, Test 2 was stopped due to safety reasons. However, the excessive shear deformations observed at the level of the damper bolts after the test (similar to Test 1) indicate that the ultimately applied vertical force was in fact close to the specimen's capacity.

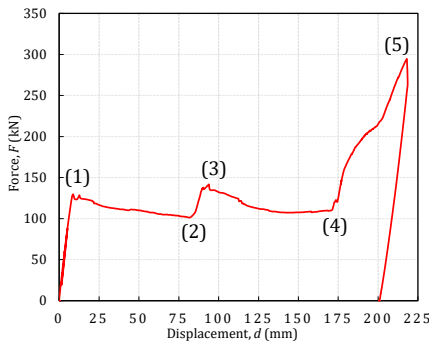


Figure 6 Test 2: Vertical load vs. displacement curve

### 3 A spring model for FREEDAM joints

#### 3.1 Modelling assumptions

Based on the well-known Component Method introduced in EN 1993-1-8 [9], a simplified two-spring model (2SM) for FREEDAM joints was developed and partially validated against experimental evidence by D'Antimo[7] and Santos et al. [10]. The model consists of two extensional springs (top and bottom) interconnected by rigid elements as represented in Figure 7. An additional rigid shear spring ensures the transfer of shear forces at the beam ends.

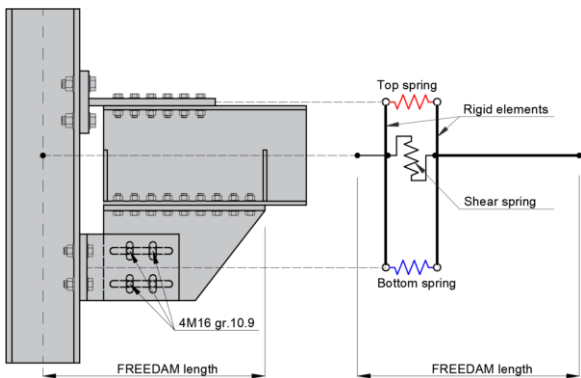


Figure 7 Simplified two-spring model (2SM) for FREEDAM joints

The so-built model accommodates the M-N interaction and accounts for the behaviour of basic joint components characterised by extensional springs with nonlinear behaviour laws (see Figure 8) derived with the Component Method of EN 1993-1-8 [9]. As demonstrated by Santos et al. [10], the component method can be effectively

extended to characterise both pre- and post-sliding behaviour of the FREEDAM joints. The plastic range of behaviour for basic joint components is characterised by a strain-hardening stiffness and an ultimate strength analytically estimated as proposed by Jaspart et al. [11].

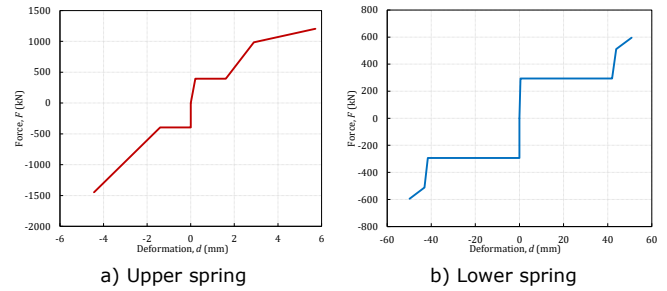


Figure 8 Behaviour laws for the two springs of the 2SM model

#### 3.2 Model validation

To validate the spring model, the experimental tests were numerically simulated using the 2SM with the spring behaviour laws given in Figure 8 combined with classical beam elements in the FINELG FE software [12]. The numerical model overlapped with the configuration of the tested specimen is schematically represented in Figure 9 for Test 1 and in Figure 10 for Test 2, respectively.

The axial restraints provided in the numerical model through extensional springs in Figure 10 simulate the in-plane experimental restraining system. The axial stiffness of these restraints was estimated at 110 kN/mm based on experimental recordings of the axial forces in the beams of the specimen and the corresponding horizontal displacement recorded at the extremities of the specimen.

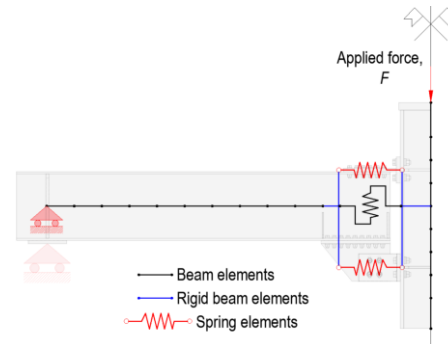


Figure 9 Schematic view of the simplified numerical model - Test 1

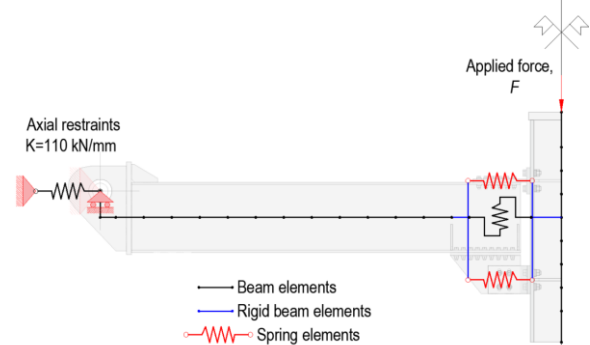
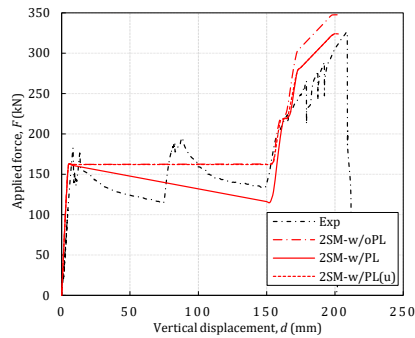
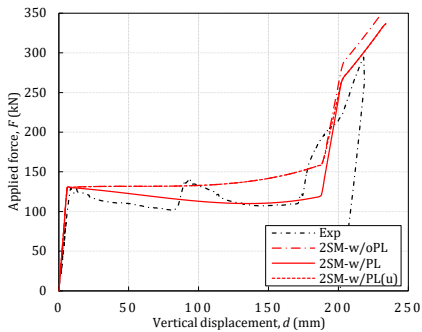


Figure 10 Schematic view of the simplified numerical model - Test 2

The prediction in terms of applied force vs. vertical displacement ( $F-d$ ) recorded during testing at the level of the column is given in Figure 11 for Test 1 and in Figure 12 for Test 2 respectively.



**Figure 11** Test 1: Predicted vertical load vs. displacement curve



**Figure 12** Test 2: Predicted vertical load vs. displacement curve

Some inconsistencies between the experimental force-displacement curve and the prediction of the 2SM are revealed in terms of overall curve shape and the ultimate capacity of the specimen. These inconsistencies arise from the approach used to characterise the behaviour of the friction damper integrated in the 2SM. The initial modelling approach used to simulate the response of the damper doesn't account for any preload loss that occurs in the preloaded high-strength (HS) M16 damper bolts along the slippage phase (2SM-w/oPL). This leads to a 6.4% overestimation of the ultimate capacity as well as to a plateau-shaped  $F-d$  curve along the slippage phase.

Nonetheless, measurements taken during Test 2 allowed concluding that an averaged 29% preload loss was registered during the slippage phase of the damper. To account for the expected preload loss, the behaviour law assigned to the lower spring of the 2SM was modified by integrating the 29% preload loss (PL) as a linear decrease along the slippage phase of the damper (w/PL behaviour law in Figure 13). However, since the resistance decay along the slippage phase due to the preload loss is not an indicative of the joint's robustness but rather a phenomenon that influences mainly the hysteretic energy dissipated under seismic excitation, an alternative characterisation of the damper was considered for robustness-related investigations. This behaviour law disregards the resistance decay along the slippage phase of the damper, yet it accounts for the effects of preload loss on the ultimate resistance of the damper assembly (see behaviour law w/PL(u) in Figure 13). Therefore, three numerical models were built with/without considering the preload loss in the bolts of the friction dampers in three different ways as indicated in Figure 13.

Figure 14 reflects the comparison between the predicted and the experimental moment-rotation curves for the right and left connections (RC and LC) of the tested joint. Generally, the 2SM shows a good performance for

predicting the full-range behaviour of the FREEDAM joints, although the results reveal the model sensitivity to the characterisation of basic joint components. Indeed, the behaviour law considered for the characterisation of the friction damper plays a crucial role in achieving accurate predictions in terms of both deformation and strength capacities.

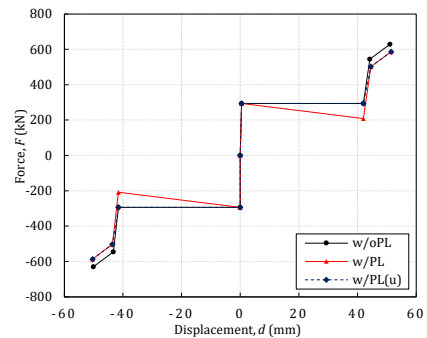


**Figure 13** Adopted behaviour laws for the damper (lower spring)

Figure 14 reflects the comparison between the predicted and the experimental moment-rotation curves for the right and left connections (RC and LC) of the tested joint. Generally, the 2SM shows a good performance for predicting the full-range behaviour of the FREEDAM joints, although the results reveal the model sensitivity to the characterisation of basic joint components. Indeed, the behaviour law considered for the characterisation of the friction damper plays a crucial role in achieving accurate predictions for both deformation and strength capacities.

It is evident that, to accurately predict the ultimate capacity of the connections, the preload loss in the damper bolts and its inherent effects on the joint's friction resistance should be considered. For both cases where the expected preload loss was considered (2SM-w/PL and 2SM-w/PL(u)), the 2SM provides predictions with acceptable accuracy for the full-range behaviour of the tested joint with a notable perfect match between the recorded and predicted ultimate moment resistance and deformation capacities, both parameters being of key importance for assessing the robustness of the joints.

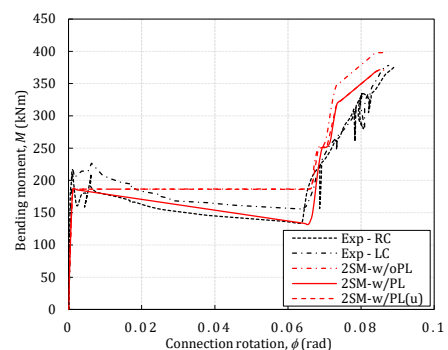


**Figure 14** Test 1: Predicted moment vs. rotation curves

The comparison between the predicted and experimental force-displacement curves for specimen 2 shown in Figure 15 reveals the sensitivity of the 2SM to the method used for characterising the behaviour of basic joint components. In particular, the best agreement between the prediction and experimentally observed response is provided by the numerical model in which the preload loss was considered as occurring along the slippage phase of the dampers with

inherent effects over the friction and ultimate resistance of the FREEDAM joints (2SM-w/PL).

The results reported in Figure 12 show that the 2SM overestimates by approximately 9% the specimen's ultimate capacity for both numerical models in which the preload loss was implemented. This discrepancy may be attributed to the fact that the experimental test was stopped due to safety reasons before reaching the actual ultimate capacity of the specimen, which corresponds to the brittle rupture of the damper bolts subjected to shear. Indeed, since the explicit failure was not reached, some residual strength should be envisaged. This was highlighted by the perfect agreement between the predicted and actual capacity of the specimen used in Test 1, where the ultimate failure was reached during the test.

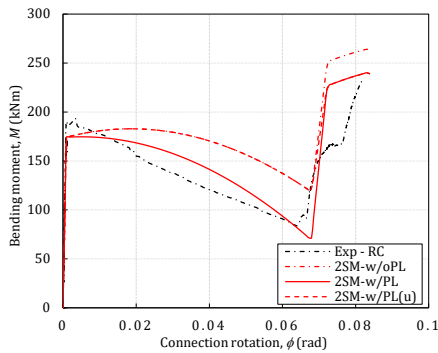


Figure 15 Test 2: Predicted moment vs. rotation curves

Figure 16 shows the development of catenary action in the beams of the specimen during testing and the predictions provided by the three numerical models. The evolution of beam axial forces seems to be insensitive to the approach chosen to characterise the response of the friction damper with respect to the bolt preload loss.

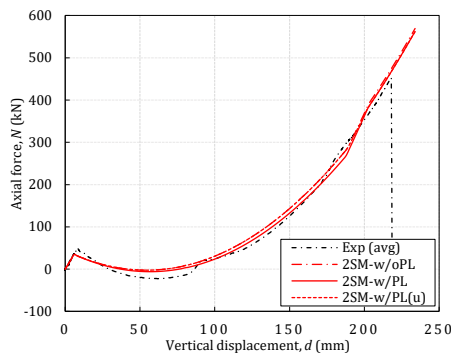


Figure 16 Test 2: Predicted beam axial force vs. displacement curves

## 4 Conclusions

Two large-scale tests were performed on dissipative FREEDAM joints extracted from the DREAMERS case study pilot building. The full range response of double-sided beam-to-column joints was experimentally assessed under two loading situations: i) monotonic bending (Test 1) and ii) a virtual column loss scenario (Test 2).

Experimental evidence highlighted the detrimental effects of the preload loss in the damper bolts during the slippage and their influence on the sliding resistance of the FREEDAM joints under quasi-static loads. Moreover, the results of the 2<sup>nd</sup> test including catenary effects revealed the capability of these joints to accommodate high levels

of displacements accompanied by the development of membrane forces in the connected beams, which proves the suitability of these joints in the context of a column loss scenario. The brittle failure mode governed by the fracture of bolts in shear, however, draws attention on the joint ductility in the post-slippage phase.

The performance of the two-spring model (2SM) proposed for the joint characterisation in numerical analyses proves its suitability for investigations in which the full-range behaviour of FREEDAM joints is of interest. Moreover, for robustness-related investigations such as simulations of column loss scenarios in which the proper integration of the post-slippage response of the FREEDAM joints is critical, the validation of the 2SM allowed identifying an acceptable compromise in terms of model complexity.

## Acknowledgements

The work presented in this paper was carried out within the DREAMERS research project (GA n°: 101034015). Financial support from the Research Fund for Coal and Steel is gratefully acknowledged.

## References

- [1] FREEDAM (2015-2018): FREE from DAMAge Steel Connections. Fund for Coal and Steel Grant Agreement No. RFSR-CT-2015-00022.
- [2] EN 1998-1, Eurocode 8 - Design of structures for earthquake resistance - Part 1: General Rules, seismic actions and rules for buildings. European Committee for Standardization, 2004.
- [3] EN 1991-1-7, Eurocode 1 - Actions on structures - Part 1-7: Accidental actions. European Committee for Standardisation, 2006.
- [4] T. Golea, A. F. Santos, J.-P. Jaspart, M. Latour, A. Santiago, and J. Demonceau, "Design for robustness of steel structures with dissipative FREEDAM joints," *International Journal of Earthquake Engineering*, vol. 2, 2022.
- [5] T. Golea, A. F. Santos, J.-P. Jaspart, M. Latour, A. Santiago, and J.-F. Demonceau, "Robustness of Steel Frame Structures Equipped with FREEDAM Dissipative Joints," *ce/papers*, vol. 5, no. 4, pp. 210–217, 2022.
- [6] R. Tartaglia, R. Carlevaris, M. D'Aniello, and R. Landolfo, "Steel Beam-to-Column Friction Joint under a Column Loss Scenario," *Buildings*, vol. 14, no. 3, Art. no. 3, Mar. 2024, doi: 10.3390/buildings14030784.
- [7] M. D'Antimo, "Impact characterization of innovative seismically designed connections for robustness application", Ph.D. Thesis, University of Liege.
- [8] ISO 6892-1:2009(E), ISO 6892-1 — Metallic materials — Tensile testing — Part 1: Method of test at room temperature. Switzerland: International Organization for Standardization, 2009.
- [9] EN 1993-1-8, Eurocode 3 - Design of steel structures - Part 1-8: Design of joints. Brussels: European Committee for Standardisation, 2005.
- [10] A. F. Santos, A. Santiago, M. Latour, G. Rizzano, and L. Simões da Silva, "Response of friction joints under different velocity rates," *Journal of Constructional Steel Research*, vol. 168, 2020.
- [11] J.-P. Jaspart, A. Corman, and J.-F. Demonceau, "Ductility assessment of structural steel and composite joints," Sep. 2019.
- [12] *FineLg user's manual*, "Nonlinear finite element analysis program." Edition 2019

